Global Change Biology

Global Change Biology (2017) **23**, 2705–2719, doi: 10.1111/gcb.13541

# Assessing forest vulnerability to climate warming using a process-based model of tree growth: bad prospects for rear-edges

RAÚL SÁNCHEZ-SALGUERO[1,2], JESUS JULIO CAMARERO[1], EMILIA GUTIÉRREZ[3], FIDEL GONZÁLEZ ROUCO[4], ANTONIO GAZOL[1], GABRIEL SANGÜESA-BARREDA[1], LAIA ANDREU-HAYLES[5,6], JUAN CARLOS LINARES[2] and KRISTINA SEFTIGEN[7]

[1]*Instituto Pirenaico de Ecología (IPE-CSIC), 50192 Zaragoza, Spain,* [2]*Departamento de Sistemas Físicos, Químicos y Naturales, Universidad Pablo de Olavide, 41013 Sevilla, Spain,* [3]*Department d' Ecologia, Universitat de Barcelona, 08028 Barcelona, Spain,* [4]*Departamento de Astrofísica y CC. de la Atmósfera, Universidad Complutense de Madrid, 28040 Madrid, Spain,* [5]*Tree-Ring Laboratory, Lamont-Doherty Earth Observatory, Palisades, NY 10964, USA,* [6] *Institut Català de Ciències del Clima (IC3), 08005 Barcelona, Spain,* [7]*Swiss Federal Institute for Forest, Snow and Landscape Research (WSL), 8903 Birmensdorf, Switzerland*

## Abstract

Growth models can be used to assess forest vulnerability to climate warming. If global warming amplifies water deficit in drought-prone areas, tree populations located at the driest and southernmost distribution limits (rear-edges) should be particularly threatened. Here, we address these statements by analyzing and projecting growth responses to climate of three major tree species (silver fir, *Abies alba*; Scots pine, *Pinus sylvestris*; and mountain pine, *Pinus uncinata*) in mountainous areas of NE Spain. This region is subjected to Mediterranean continental conditions, it encompasses wide climatic, topographic and environmental gradients, and, more importantly, it includes rear-edges of the continuous distributions of these tree species. We used tree-ring width data from a network of 110 forests in combination with the process-based Vaganov–Shashkin-Lite growth model and climate–growth analyses to forecast changes in tree growth during the 21st century. Climatic projections were based on four ensembles $CO_2$ emission scenarios. Warm and dry conditions during the growing season constrain silver fir and Scots pine growth, particularly at the species rear-edge. By contrast, growth of high-elevation mountain pine forests is enhanced by climate warming. The emission scenario (RCP 8.5) corresponding to the most pronounced warming (+1.4 to 4.8 °C) forecasted mean growth reductions of −10.7% and −16.4% in silver fir and Scots pine, respectively, after 2050. This indicates that rising temperatures could amplify drought stress and thus constrain the growth of silver fir and Scots pine rear-edge populations growing at xeric sites. Contrastingly, mountain pine growth is expected to increase by +12.5% due to a longer and warmer growing season. The projections of growth reduction in silver fir and Scots pine portend dieback and a contraction of their species distribution areas through potential local extinctions of the most vulnerable driest rear-edge stands. Our modeling approach provides accessible tools to evaluate forest vulnerability to warmer conditions.

*Keywords:* *Abies alba*, climate change, dendroecology, emission scenarios, forward growth model, *Pinus sylvestris*, *Pinus uncinata*, Vaganov–Shashkin-Lite model

*Received 15 June 2016; revised version received 17 October 2016 and accepted 18 October 2016*

## Introduction

Climate is one of the major filters determining where a specific tree species can thrive (Pearson & Dawson, 2003). Hence, the variation in climate along geographical gradients allows analyzing how forest growth and productivity change in response to environmental variation (Babst *et al.*, 2013; Martin-Benito & Pederson, 2015). Specifically, characterizing forest growth patterns along climatic gradients has a great potential to project the vulnerability of tree populations to climate warming (Matías & Jump, 2015; Shestakova *et al.*, 2016). Several lines of evidence indicate that rising atmospheric $CO_2$ concentrations and associated climate warming will further alter the growth, functioning and distribution of forests in drought-prone areas over the coming decades (Keenan *et al.*, 2011; Linares & Camarero, 2012a,b). Changes in forest productivity and range shifts of major tree species will have economic, ecological and social impacts, especially if accompanied by widespread dieback of the most vulnerable stands (Allen *et al.*, 2015; Anderegg *et al.*, 2015).

In drought-prone areas, climate warming can influence forests by modifying the start and duration of the growing season and by rising evapotranspiration rates, thus amplifying drought stress and triggering forest dieback (Williams *et al.*, 2013; Camarero *et al.*, 2015b;

Correspondence: Jesus Julio Camarero, tel. +34 976 716031, fax +34 976 716019, e-mail: jjcamarero@ipe.csic.es

Guada *et al*., 2016). However, even though forests play a key role in the global C cycle and sequestration of carbon emissions derived from fossil fuels (Way & Oren, 2010), there are still research gaps on how rising temperatures will affect tree growth under projected climatic conditions. Special attention must be paid to tree populations located at the lower latitudinal and altitudinal limit of the trees species' continuous distribution area (rear-edge, cf. Hampe & Petit, 2005), where water availability becomes the main constraint of forest growth (Sánchez-Salguero *et al*., 2012). In this sense, new approaches are needed to assess forest vulnerability in response to predicted climate warming, and tree-ring data can provide a long-term assessment of forest productivity by quantifying growth changes (Babst *et al*., 2014). Comparing forest growth responses to observed and forecasted climate projections along ample geographical gradients, including rear-edge tree populations, should improve our ability to model forest vulnerability to climate warming (Huang *et al*., 2013).

Most modeling efforts have focused on the impacts of climate change on tree species distributions (D'Amen *et al*., 2015; García-Valdés *et al*., 2015), but few studies have evaluated forest vulnerability to climate warming using growth models (but see Serra-Díaz *et al*., 2013; Duveneck & Scheller, 2016). The development of process-based forward models of tree-ring formation offers a valuable tool for understanding forest growth responses to climate (Anchukaitis *et al*., 2006; Evans *et al*., 2006; Guiot *et al*., 2014). The Vaganov–Shashkin-Lite model (hereafter VS-Lite model; Vaganov *et al*., 2006, 2011; Tolwinski-Ward *et al*., 2011, 2013) is one of the best and simplest available models for understanding the nature of growth response to climate across regional scales (Breitenmoser *et al*., 2014). This process-based model simulates radial growth using the principle of limiting factors and nonlinear growth response functions (Fritts, 2001), and it requires the following as input variables: site latitude, monthly mean temperature, and monthly total precipitation. The VS-Lite model has been used to successfully simulate and evaluate regional patterns of climate limitation of tree growth in a range of environments from semi-arid to temperate and boreal regions (Tolwinski-Ward *et al*., 2011; Breitenmoser *et al*., 2014; Lavergne *et al*., 2015; Mina *et al*., 2016).

Here, we assess radial growth as a function of different climate projections under four emission scenarios (IPCC, 2013) using the VS-Lite model and statistical climate–growth models. Particularly we considered the 'representative concentration pathways' (RCPs) which are climate projections consistent with a wide range of possible changes in future anthropogenic greenhouse gas emissions (Collins *et al*., 2014). We focus on three keystone conifer species abundant in boreal, subalpine, temperate and Mediterranean areas of Europe: silver fir (*Abies alba* Mill.), Scots pine (*Pinus sylvestris* L.) and mountain pine (*Pinus uncinata* Mill.). The three species reach the southernmost distribution limit of their continuous distribution area in Spain, a vulnerable region to climate warming as drought-induced dieback episodes have already been observed in silver fir and Scots pine populations (Camarero *et al*., 2015b). In this Mediterranean region, warming is projected to enhance aridity, exacerbating soil moisture deficit and increasing the vapor pressure deficit (Giorgi & Lionello, 2008). Although the drought and temperature sensitivity of tree growth has been documented in some forests of this area (Andreu *et al*., 2007; Galván *et al*., 2012; Gazol *et al*., 2015), the vulnerability to forecasted climate warming has not been investigated, particularly in the case of rear-edge populations.

Specifically, we are interested in investigating whether climate-based models of growth could be used to identify vulnerability thresholds of forests reflected as growth reductions. We also evaluate the long-term growth responses of rear-edge forests to climate warming at the species, site and tree levels. Our specific objectives are the following: (1) to characterize growth responses to climate across wide environmental and geographical gradients including rear-edge forests; (2) to calibrate climate–growth relationships using a process-based model of tree-ring formation; (3) to explore the vulnerability of forests under different forcing climatic scenarios. We hypothesize that rear-edge forests of drought-sensitive species (silver fir and Scots pine) will be the most vulnerable to a warming-induced decrease in water availability, whereas rising temperatures will enhance growth and growing season duration of high-elevation mountain pine forests.

## Materials and methods

### *Study sites and species*

The study area includes the main mountain ranges of NE Spain, namely the Pyrenees and the Iberian System (Fig. 1; see also Fig. S1 in Supporting Information). The Pyrenees constitute a transitional area between more humid conditions in their northern margin and drier conditions southward (Vigo & Ninot, 1987). This gradient overlaps with a longitudinal gradient caused by the location of the range between the Atlantic Ocean and the Mediterranean Sea leading to higher winter–spring and summer–fall precipitation amounts westward and eastward, respectively. The climate in the Pyrenees is continental with oceanic (western sites) or Mediterranean (eastern and southern sites) influences (Figs S1 and S2, Table S1). The Iberian range is subjected to Mediterranean climate with a continental influence, characterized by warm and dry summers and

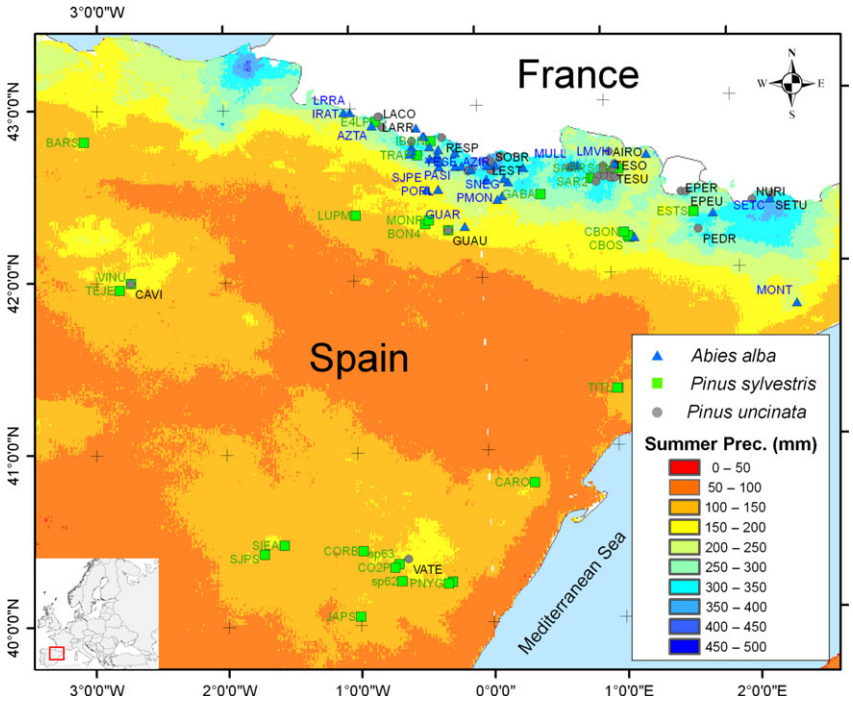


**Fig. 1** Map showing the sites of the three tree species studied in NE Spain (silver fir, *Abies alba*, blue triangles; Scots pine, *Pinus sylvestris*, green squares; and Mountain pine, *Pinus uncinata*, dark gray circles) and summer precipitation (color background area). (See Table S1 and Fig. S1 for more details on the sampled sites and species distribution.) The inset shows the location of the study area in Europe. [Colour figure can be viewed at wileyonlinelibrary.com].

cool winter conditions (Camarero *et al.*, 2015b). Mean annual temperature and total precipitation in the study sites range from 3.0 to 15.4 °C and from 460 to ca. 1800 mm, respectively, with January and July as the coldest and warmest months, respectively (Galván *et al.*, 2012). Since 1950, warmer conditions have been observed in NE Spain (Fig. S2).

Silver fir appears in the wettest sites of the study area usually dominating in N-oriented sites with deep soils (Camarero *et al.*, 2011). Scots pine appears in the driest and warmest sites of the area, whereas mountain pine abounds in the coldest and high-elevation sites forming the Pyrenean tree line (Vigo & Ninot, 1987). The sampled sites encompass the maximum ecological amplitude of the species for the study region by including silver fir and Scots pine dominant in low to middle elevations (range 850–2000 m, mean elevation 1480 m) and mountain pine forests dominant at higher elevations (1750–2451 m, mean elevation 2113 m; see Table S1). Note that some geographical variables covary because elevation of sampled sites decreases westward and southward, especially in the case of silver fir and mountain pine forest. Most sampled sites are located inside protected areas (National and Regional parks) which guarantee that trees have been less exposed to local perturbations (logging, fire) than in nonprotected areas for the past 60 years. Pyrenean sites are either located on marl or limestone substrates, which generate basic soils (mainly silver fir forests), or on moraine deposits with rocky and acid soils (mainly pine forests), while the remaining sites are characterized by basic and clayey or loamy soils (Camarero *et al.*, 2015a,b,c).

### *Tree-ring dataset*

Between 1994 and 2015, 110 sites were sampled distributed as follows: silver fir ($n$ = 45 sites), mountain pine ($n$ = 37 sites) and Scots pine ($n$ = 28 sites) (Table S1). We sampled these sites following dendrochronological methods and covering most of the geographical distribution of the three species in the Iberian Peninsula, thus capturing most of the ecological variability experienced by these species (Fig. S1 and Table S1). At each site, at least 15 standing dominant or codominant trees, separated by at least 20 m from each other, were selected and the latitude and longitude of the site were recorded (Table S1) (Nehrbass-Ahles *et al.*, 2014). Topographic (elevation, slope and aspect) variables were also recorded for each tree. Most study sites are relatively undisturbed and they have not been logged since the 1950s (Camarero *et al.*, 2011). Radial growth was measured in two to three radial cores per tree, which were extracted with an increment borer at breast height (1.3 m) on the cross-slope sides of the trunk whenever possible (Fritts, 2001). Wood samples were sanded until rings were visible and then visually cross-dated. Once dated, the tree-ring widths were measured to the nearest 0.01 mm using a binocular microscope and a LINTAB measuring device (Rinntech, Heidelberg, Germany). The accuracy of visual cross-dating and measurements was checked with the COFECHA program, which calculates moving correlations between each individual series and the mean site series (Holmes, 1983).

To quantify the growth–climate associations, we developed both mean tree-ring width series at the tree and site levels (site

chronology) (Table S2). Tree-ring width indices (hereafter abbreviated as TRWi) were calculated using the ARSTAN program (ver. 4.4; Cook & Krusic, 2005). We adjusted negative exponential or linear functions and 25-year long splines to obtain the detrended TRWi series correcting the age/size trends. These relatively short splines remove growth trends in periods longer than decades, with holding the high-frequency growth variability. We applied autoregressive models to model and eliminate the temporal (usually of first order) autocorrelation. Finally, we obtained TRWi series for each tree as ratios between the measurement and the fitted curve. Among the developed chronologies, we considered only those covering the period 1950–2005, which corresponded to the period of most reliable climatic data in the study area. Finally, we averaged the individual growth-index series into site-level chronologies following a hierarchical approach from tree to site. To characterize the growth series at the site level, we also calculated several dendrochronological statistics considering raw data (Table S2) and enabled the evaluation of the validity of the tree-ring chronologies (Fritts, 2001).

### *Climate: current observations and future projections*

The homogenized and quality-checked E-OBS v.11.0 dataset was used for period 1950–2005 providing a reliable climatic data source across the whole study area (Haylock *et al.*, 2008). This dataset contains monthly mean temperature and precipitation data gridded at a 0.25° spatial resolution which have been checked for homogeneity. Only those climate variables highly correlated with TRWi were considered in the climate-based models and TRWi projections under different climate scenarios.

The climate data projected for the 21st century was downloaded and downscaled (cf. Moreno & Hasenauer, 2016) at a 0.25° spatial resolution from the fifth phase of the Coupled Model Intercomparison Project (ensemble CMIP5; Taylor *et al.*, 2012). We used data for the scenario (RCP 8.5) that most closely tracked recent historical emissions (Lelieveld *et al.*, 2016), and three lower emissions scenarios in which the increase in annual emissions is more gradual in the early 21st century and declines after the mid-21st century (RCP 2.6, RCP 4.5 and RCP 6.0). These scenarios result in 1.7–4.8 °C global warming by the year 2100, relative to the late-20th-century baseline (Fig. S3). The RCP 2.6 scenario represents a situation where radiative forcing peaks at 3.0 W $m^{-2}$ before 2100 and then declines to reach 2.6 W $m^{-2}$ by 2100 with warming increase ranging between 0.3 and 1.7 °C during 21st century. In the RCP 4.5 scenario, radiative forcing stabilizes at 4.5 W $m^{-2}$ after 2100 with temperature increase ranging between 0.9 and 2.6 °C. In the RCP 6.0 scenario, radiative forcing stabilizes at 6.0 W $m^{-2}$ after 2100 with warming increase ranging between 0.8 and 3.1 °C, whereas in the RCP 8.5 scenario, radiative forcing continuously rises to reach 8.5 W $m^{-2}$ in 2100 with warming increase ranging between 1.4 and 4.8 °C (Van Vuuren *et al.*, 2011).

### *Forward process-based model of tree growth*

We used the VS-Lite model and a Bayesian parameter estimation approach to simulate TRWi as a function of climate (Tolwinski-Ward *et al.*, 2011, 2013). The model uses the Leaky Bucket model of hydrology provided by the National Oceanic and Atmospheric Administration's Climate Prediction Centre (Huang *et al.*, 1996) to estimate monthly soil moisture from temperature and total precipitation data. Snow dynamics are not considered in the model, and thus, all precipitation is assumed to be liquid. For each year, the model simulates standardized tree-ring width anomalies from the minimum of the monthly growth responses to temperature ($gT$) and moisture ($gM$), modulated by insolation ($gE$). Day length is determined from site latitude and does not vary from year to year. The growth response functions for temperature ($gT$) and moisture ($gM$) in VS-Lite involve only two parameters. The first parameter represents the temperature ($T_1$) or moisture ($M_1$) threshold below which growth will not occur, while the second is the optimal temperature ($T_2$) or moisture ($M_2$) above which growth is not limited by climate. The growth function parameters were estimated for each site via Bayesian calibration. This scheme assumes uniform priors for the growth response parameters and independent, normally distributed errors for the modeled TRWi values. The posterior median for each parameter was used to obtain the 'calibrated' growth response for a given site. Finally, the model was run over the entire period 1950–2005 using the calibrated parameters for each site to produce a simulated tree-ring chronology (TRWi-$_{VSL}$) that represents an estimate of the site climate signal of forest growth. A more detailed description of the approach can be found in the study by Tolwinski-Ward *et al.* (2013).

Temperature ($T_i$) and soil moisture ($M_i$) growth parameters were sampled uniformly across intervals, and the growth parameter set producing the simulation that correlated most significantly with the corresponding observed TRWi series for each site was then used in the simulations. In addition, other parameters (e.g., soil moisture, runoff, root depth) were taken from published studies (e.g., Evans *et al.*, 2006; Vaganov *et al.*, 2006; Tolwinski-Ward *et al.*, 2011, 2013; Touchan *et al.*, 2012). The model was evaluated 12 000 times for each site using three parallel Markov chain Monte Carlo chains with uniform prior distribution for each parameter and a white Gaussian noise model error (Tolwinski-Ward *et al.*, 2013). To compute annual TRWi values, we integrated the overall simulated growth rates (i.e., the point-wise minimum of monthly $gT$, $gM$ and $gE$) over the time window from September of the year prior to growth to October of the year of tree-ring formation. This period was determined following previous xylogenesis and dendroecological studies performed on the three species (Camarero *et al.*, 1998; Tardif *et al.*, 2003). To evaluate the temporal stability of the calibrated growth response functions, we divided the period 1950–2005 into two 25-year intervals (1950–1980, 1975–2005) and withhold the second half for validation of the parameters estimated in the first half (Fig. S4 and Table S3).

### *Climate–growth relationships and growth forecasts*

To characterize the geographical variation in growth of the three species across space and time, we conducted a non-metric multidimensional scaling (NMDS), which is a multidimensional analysis effective in quantifying the relationships

between climate and TRWi (Oberhuber, 2004). The NMDS was applied to the entire network of observed TRWi chronologies for the 1950–2005 period and also to the TRWi values projected for the 2050–2100 period.

The relationships between monthly climate data (mean temperatures and precipitation) and TRWi were assessed by calculating Pearson correlation coefficients for the common period 1950–2005. The temporal window of growth–climate comparisons included from the previous September up to the current October. These climate–growth relationships were reexamined by applying stepwise multiple linear regressions to identify the effects of climate on the observed TRWi data and to project TRWi through individual site climate-based equations. Monthly climatic variables for each site were transformed into normalized standard deviations to give them the same weight in the fitted models. We used the function *step* of the R package *stats* (R Development Core Team, 2016) using the lowest Akaike information criterion for selecting the final regression equations. The models were fitted using generalized least-squares estimation (GLS) and the R package *nlme* (Pinheiro *et al.*, 2009). The selected models were run to forecast the TRWi of each site (hereafter $TRWi_p$) for the 2001–2049 and 2050–2100 periods under the RCPs scenarios. Finally, we conducted VS-Lite models on $TRWi_p$ series over the same periods to forecast growth responses (i.e., $gT$, $gM$) and growth function parameters ($T_1$, $T_2$ and $M_1$, $M_2$) under future climate projections.

## Results

### *Climate–growth relationships: site variability and species-specific patterns*

We detected a high site-to-site variability in the climate–growth relationships within each tree species (Fig. 2). We found a common significant influence of previous September climate conditions on silver fir, positively and negatively related to high precipitation and temperature, respectively. This negative association with drier conditions during the previous late summer augmented as elevation decreased (Pearson correlation: $r = 0.50$, $P < 0.01$) and intensified in driest rear-edge sites (e.g., GUAR site). Warm February and April temperatures were positively related to silver fir growth, and this effect increased with elevation in the case of February ($r = 0.28$, $P < 0.05$). Current wet May–July conditions were positively related to silver fir TRWi, especially at low-elevation sites. In contrast, the negative relationship of June–July temperature and TRWi increased with elevation.

Scots pine TRWi positively responded to high May–July precipitation, especially at low elevations ($r = -0.60$, $P < 0.05$) but also eastward. The significant limiting effect of warm June–July temperatures on growth decreased westward ($r = -0.52$) and upward, whereas warm and dry conditions in the previous late summer were associated with lower TRWi values, particularly at low elevations.

Mountain pine TRWi were positively related to warm conditions during previous October–November and current April–May temperature, and the former association reinforced upward ($r = 0.36$, $P < 0.05$). Lastly, July precipitation was significantly and positively related to TRWi only in the case of the rear-edge VATE site ($r = 0.34$).

### *Assessment of the process-based growth projections*

The VS-Lite model accurately predicted the year-to-year variability in TRWi during the 1950–2005 period (Fig. S4). Mean correlation coefficients between observed and simulated TRWi values were significant in all sites (see Table S3 and Fig. S4).

The modeled growth response to temperature ($gT$) and soil moisture ($gM$) differed among sites and species (Fig. 3a). The mean growth response to temperature ($gT$) peaked from July to August, while the growth response to moisture ($gM$) dropped during summer as expected in response to high evapotranspiration rates and soil moisture deficit. Tree growth was limited by low temperatures ($gT < gM$) at the beginning and end of the growing seasons and by soil moisture availability ($gM < gT$) during summer and autumn (from July to September in silver fir; from June to October in Scots pine; see Figs 2 and 3). In contrast to these two moisture-sensitive species, mountain pine growth was mainly limited by low temperatures. There were exceptions to the mountain pine pattern such as the growth constrain by low summer moisture in the rear-edge VATE site (Fig. S5). Similarly, some of the driest rear-edge silver fir (e.g., GUAR) and Scots pine (e.g., CORB) sites also presented moisture-limited growth response (Fig. S5).

The estimated minimum and optimal thresholds ($T_1$, $T_2$ and $M_1$, $M_2$) for growth confirmed the highest sensitivity of mountain pine growth to cold temperatures (maximum $T_2$ value) and that of silver fir to low soil moisture values (maximum $M_2$ value; see Table S4). Nevertheless, it is necessary to consider that these are mean parameters for the whole studied distribution which vary as a function of site features related to geographical location and elevation (Fig. S6).

### *Modeling growth as a function of climate*

The selected climate-based GLS models explained on average 64%, 68% and 75% of the TRWi variance in silver fir, Scots pine and mountain pine sites, respectively. The number of climate predictors entering the GLS models ranged from 3 to 10 (Table S5). These predictors were similar to the most influential monthly climate variables detected in the analyses of climate–growth relationships (Fig. 2). The predicted TRWi series based on GLS

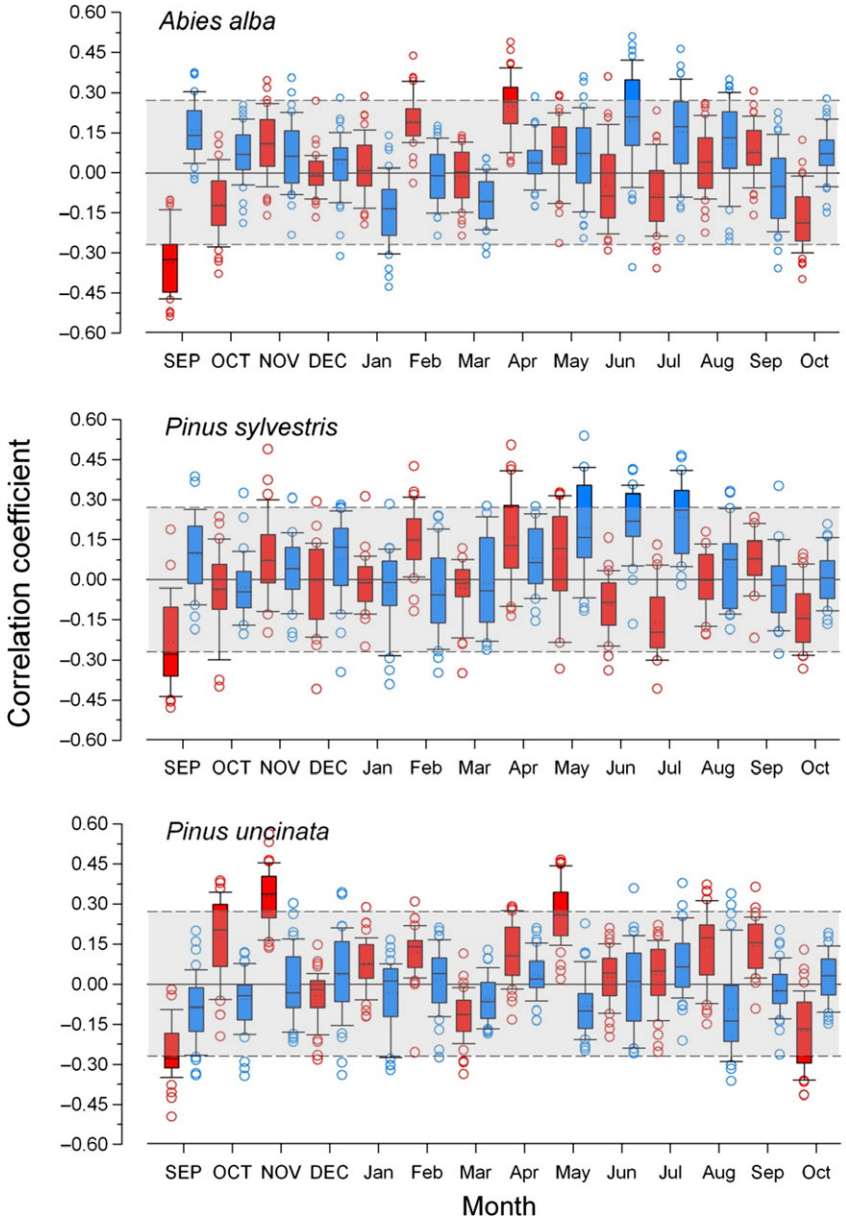


**Fig. 2** Pearson correlation coefficients calculated between site chronologies of tree-ring width indices and mean temperature (red bars) and total precipitation (blue bars) for the three study species (silver fir, *Abies alba*; Scots pine, *Pinus sylvestris*; and Mountain pine, *Pinus uncinata*) and for the common period 1950–2005. Each box shows the 25th and 75th percentiles of correlations (lower and upper edges of boxes, respectively), the median (thin line) correlation values. The outliers located below and above the 5th and 95th percentiles are also displayed. The analyzed temporal window spans from previous September up to current October. The values located outside the gray box and dashed lines indicate significant ($P < 0.05$) correlation coefficients. [Colour figure can be viewed at wileyonlinelibrary.com].

climate–growth models were within the range of the observed TRWi values for the 1950–2005 period (Figs 4 and S7).

### *Projected growth responses to climate warming*

Under the warmest climate scenario (RCP 8.5), silver fir and Scots pine tree growth is predicted to be increasingly constrained by soil moisture availability ($gM < gT$), thus experiencing more drought stress during the growing season (Fig. 3b). In the case of mountain pine, models predict an extended growing season (from late winter to late autumn season) during the second half of 21st century. Under the different forcing scenarios, a longer dry season limitation would negatively affect the growth of silver fir and Scots pine,

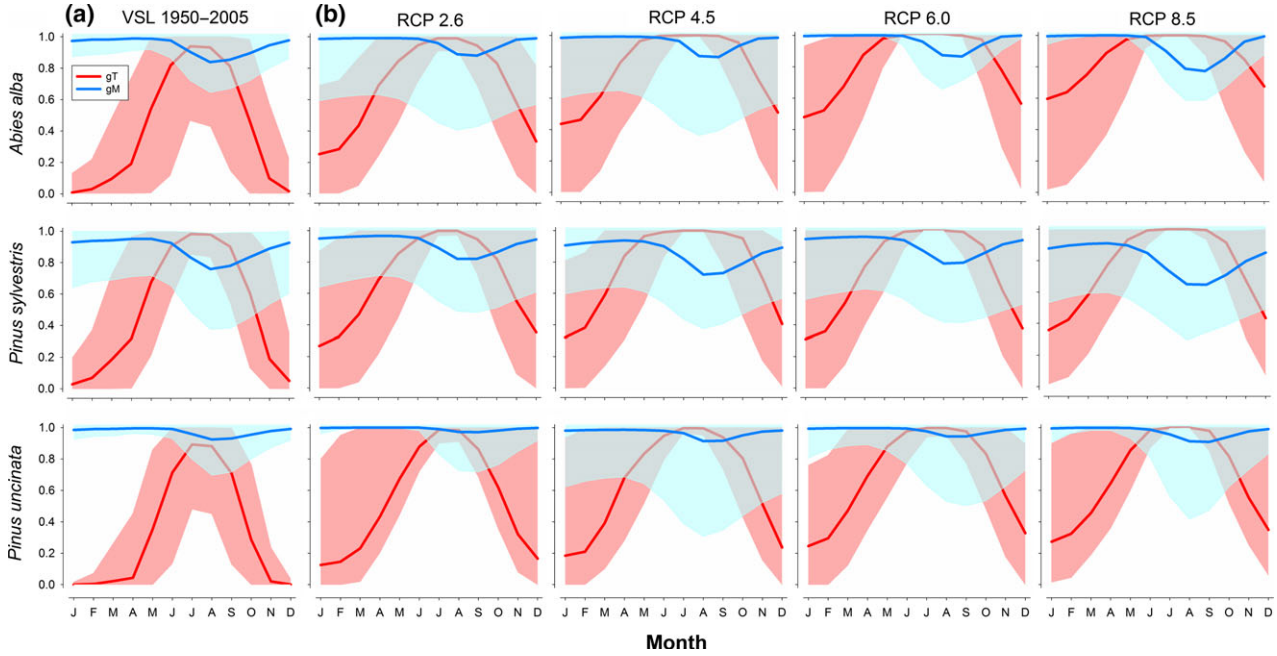


**Fig. 3** Simulated (VS-Lite, period 1950–2005) and projected monthly growth response curves considering temperature (*gT*, red lines – mean and areas – range sites) and soil moisture limitations (*gM*, blue lines – mean and areas – range sites) for each tree species (a). Projected growth response curves correspond to the IPCC AR5 emission scenarios (from lowest to highest rates of warming: RCP 2.6, RCP 4.5, RCP 6.0 and RCP 8.5) for the period 2050–2100 (b). [Colour figure can be viewed at wileyonlinelibrary.com].

especially at dry rear-edge sites located southward or at low elevation which would become very vulnerable to further warming and amplified drought stress (Fig. S5).

The warmer and drier conditions projected by the scenario tracking recent historical emissions (RCP 8.5) forecasted a TRWi reduction in silver fir and Scots pine during the late 21st century being this growth decline most pronounced since 2050 (Figs 4 and S7). Contrastingly, mountain pine TRWi would increase until 2100. Considering the three species, on average a weak decrease in TRWi is projected for the near future (2001–2049) compared to the reference 1950–2005 period (Table 1). In contrast, TRWi declines are forecasted for the RCP 8.5 scenario in Scots pine (−16.4%) and silver fir (−10.7%) forests for the 2050–2100 period, whereas a growth enhancement is expected for mountain pine (+12.5%).

The projected changes in TRWi vary across sites (Table 1), following the above-mentioned geographical and altitudinal patterns (Figs 6 and S6). The NMDS biplots of observed TRWi displayed silver fir and mountain pine sites along the first axis (NMDS1), related to elevation, whereas Scots pine sites showed more dispersion along the second axis (NMDS2) associated with latitude and longitude (Figs 5 and S8). Rear-edge sites were mainly located at the periphery of the biplot indicating different climate–growth associations as compared with the rest of sites. These marginal positions of the rear-edge sites in the NMDS biplot were even more extreme in the case of Scots pine when subjected to the warmest climate scenario (RCP 8.5).

Most silver fir sites would show decreasing TRWi trends (Fig. 6), and the strongest reductions are forecasted to occur in western and low-elevation sites as the rear-edge GUAR site (Figs 6 and S7). In Scots pine, TRWi-negative trends were mainly detected in southward low-elevation sites where drought stress is expected to intensify. Lastly, in mountain pine, TRWi-positive trends were more prominent northward and at high elevation where cold temperatures most constrain growth, excepting in the case of the negative trends observed in the rear-edge VATE site (Figs 6 and S7).

### *Changes in the climatic thresholds of growth*

We observed an increase in the minimum temperature threshold of growth ($T_1$) in silver fir and a rise in the optimum temperature growth thresholds ($T_2$) in Scots pine for the 2050–2100 period (Fig. 7 and Table S6). Concomitantly, the estimated minimum soil moisture for growth ($M_1$) would increase for both tree species; however, the optimum soil moisture for growth ($M_2$) would decrease significantly only in silver fir. Thus, growing conditions would sharply deteriorate because of a declining supply of soil water, being this water

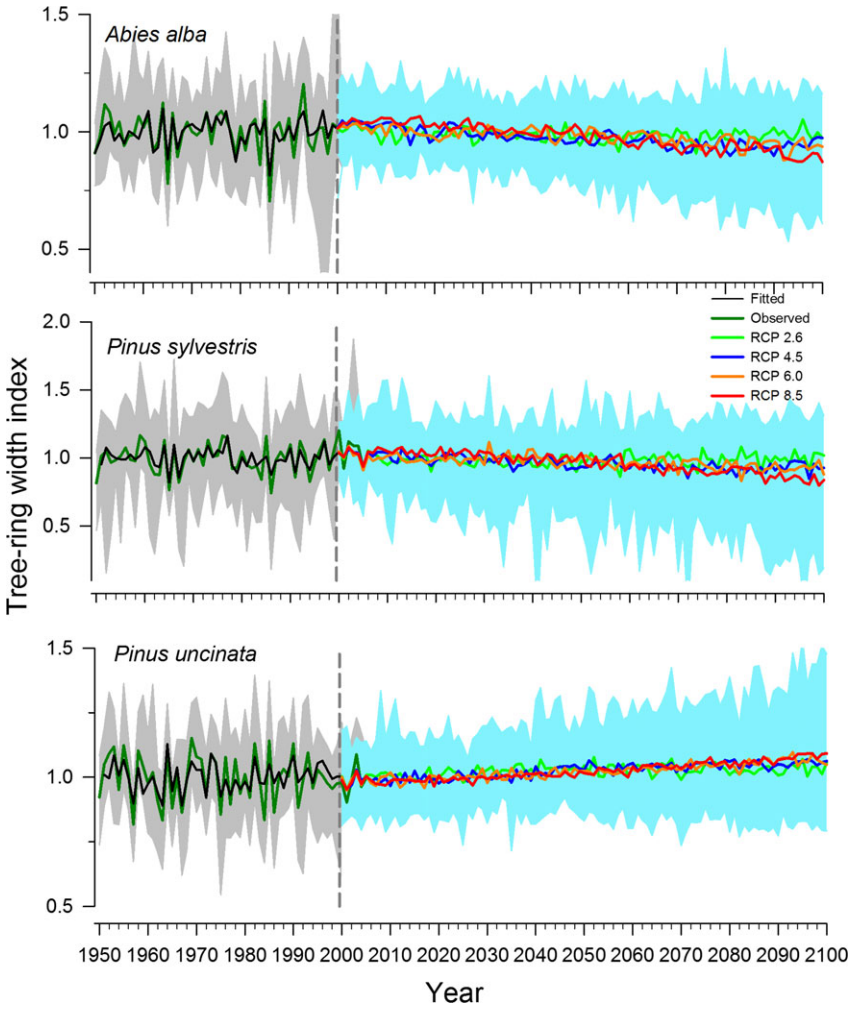


**Fig. 4** Observed (period 1950–2005) and projected (period 2001–2100) tree-ring width indices (TRWi) for each tree species (silver fir, *Abies alba*; Scots pine, *Pinus sylvestris*; and Mountain pine, *Pinus uncinata*). Means are shown as dark green lines and gray, and cyan polygons represent the TRWi maximum and minimum values considering all sites. Projections are based on IPCC AR5 considering the RCP 2.6 (green), RCP 4.5 (blue), RCP 6.0 (orange) and RCP 8.5 (red) emission scenarios. [Colour figure can be viewed at wileyonlinelibrary.com].

limitation more pronounced in some rear-edge sites (Figs S5, S7 and S8). In contrast, mountain pine growth projection scenarios are characterized by warmer temperature thresholds, but also smaller optimum soil moisture conditions ($M_2$) regardless of the emission scenario (Fig. 7 and Table S6), and this trend is especially marked again at rear-edge sites (e.g., CAVI; Fig. S5).

## Discussion

Understanding the temporal and spatial growth variability in response to climate is fundamental to assess forest vulnerability to forecasted climate warming. Our projections based on a process-based model of tree growth demonstrate that the impacts of climate warming on forests depend on the tree species' vulnerability to warmer and drier conditions, which is illustrated by the responses of dry rear-edge sites. So far as we know, the forest growth vulnerability to climate warming has not been fully investigated across driest rear-edges of several keystone tree species, at least in the case of Europe (Lindner *et al.*, 2010). In addition to the geographical and altitudinal trends in the species-specific growth–climate relationships (Figs 2, 6 and S6) observed in the study area, there exists a relevant site variability modulating forest vulnerability thresholds (Galván *et al.*, 2012; Gazol *et al.*, 2015). Such local gradients reproduce to some extent rear-, optimum and leading-edge conditions, representing geographical analogues of forest growth under forecasted warming scenarios (cf. Ruosch *et al.*, 2016). Our combination of

**Table 1** Modeled percentage change in average tree-ring width (TRWi) for projected climate change trends ($TRWi_p$) considering the ensemble IPCC AR5 emission scenarios (RCP 2.6, RCP 4.5, RCP 6.0 and RCP 8.5). Values are calculated such as the projected 2001–2049 and 2050–2100 annual mean minus measured 1950–2000 annual mean

| | 2001–2049 | | | | 2050–2100 | | | |
|---|---|---|---|---|---|---|---|---|
| | Emission scenarios | | | | Emission scenarios | | | |
| Tree species | RCP 2.6 | RCP 4.5 | RCP 6.0 | RCP 8.5 | RCP 2.6 | RCP 4.5 | RCP 6.0 | RCP 8.5 |
| Silver fir (*Abies alba*) | | | | | | | | |
| Mean | −1.8 | −0.9 | −1.7 | 2.4 | −4.1 | −7.8 | −9.2 | −10.7 |
| SD | 1.7 | 0.7 | 0.6 | 1.6 | 3.9 | 5.6 | 4.5 | 5.2 |
| Max | 1.2 | 0.5 | 0.8 | 5.1 | 1.9 | 8.5 | −3.3 | −2.7 |
| Min | −6.2 | −2.8 | −1.6 | −0.6 | −11.5 | −17.2 | −16.7 | −20.9 |
| Scots pine (*Pinus sylvestris)* | | | | | | | | |
| Mean | −2.9 | −1.7 | −1.2 | 2.5 | −5.9 | −11.3 | −11.1 | −16.4 |
| SD | 3.6 | 1.5 | 0.9 | 3.4 | 5.1 | 8.5 | 7.4 | 11.9 |
| Max | 2.9 | 2.8 | −0.3 | 9.1 | 3.2 | −2.6 | −3.1 | −5.1 |
| Min | −10.8 | −4.2 | −3.5 | −3.2 | −16.6 | −31.9 | −27.8 | −40.6 |
| Mountain pine (*Pinus uncinata*) | | | | | | | | |
| Mean | 1.3 | 0.9 | −0.5 | −1.1 | 3.5 | 6.1 | 8.7 | 12.5 |
| SD | 2.2 | 1.1 | 0.8 | 1.1 | 6.6 | 7.5 | 7.4 | 7.7 |
| Max | 6.7 | 2.4 | 1.5 | 1.2 | 21.2 | 23.1 | 23.5 | 29.7 |
| Min | −4.1 | −2.8 | −2.7 | −4.3 | −11.2 | −13.7 | −11.5 | −13.8 |

biogeographical and dendroecological information with process-based modeled growth complements previous findings based only on niche-based models (Lloret *et al*., 2013; Serra-Díaz *et al*., 2013; García-Valdés *et al*., 2015) by demonstrating the presence of contrasting responses to observed and forecasted climate trends among tree populations.

The projected warming trends will have contrasting effects on the performance of silver fir and Scots pine across its southernmost distribution areas (Figs 4 and 5) which agrees with recent observations of growth decline in some of these sites (Macias *et al*., 2006; Andreu *et al*., 2007; Gazol *et al*., 2015). We found evidences suggesting an expected growth decline at rear-edge sites where climate tolerance is low (Figs 5 and 6) and a notable growth improvement in cold-limited mountain pine forests which also agrees with previous findings (Galván *et al*., 2012).

### *Projected growth responses to different warming intensities*

Forecasted warmer and drier conditions led to growth decline which would be more intense on the southern and lower elevation sites where growth is most sensitive to precipitation (Figs 3–6). On the contrary, warmer conditions would lengthen the growing season of high-elevation mountain pine sites where growth enhancement is predicted. The magnitude and speed at which these changes might occur depend on climate forcing and timescales, with fastest and greater growth shifts (Figs 4 and 6) occurring under the most rapidly warming RCP 8.5 scenario (Ruosch *et al*., 2016). The most substantial impacts on growth are predicted to be negative for several rear-edge silver fir and Scots pine forests which agrees with late 20th-century reports of drought-triggered growth decline (Martínez-Vilalta & Piñol, 2002; Macias *et al*., 2006; Camarero *et al*., 2015b). For instance, large growth reduction would occur at rear-edge sites as TITL (−35.5%) in the case of Scots pine or GUAR (−19.2%) in the case of silver fir (Fig. 5). Note that forest dieback in response to severe droughts during the late 20th century has already been reported in some of these sites (Camarero *et al*., 2011, 2015b). This could translate into changes in species composition of these forests (Galiano *et al*., 2011).

These projections imply that some Scots pine and silver fir rear-edge forests could not compensate for the growth decline forecasted during the late 21st century under the RCP 8.5 scenario. As many rear-edge stands (e.g., TITL and GUAR sites) are located in mountainous areas which represent 'cold islands' surrounded by Mediterranean dry conditions in the lowlands, we expect that upward shifts would be more feasible than northward displacements requiring very long dispersal events in a region where land use and climate preclude this migration type. Nevertheless, it is not clear whether tree species will be able to track future climate warming, and range contractions seem a plausible scenario for southernmost margins (Zhu *et al*., 2012).

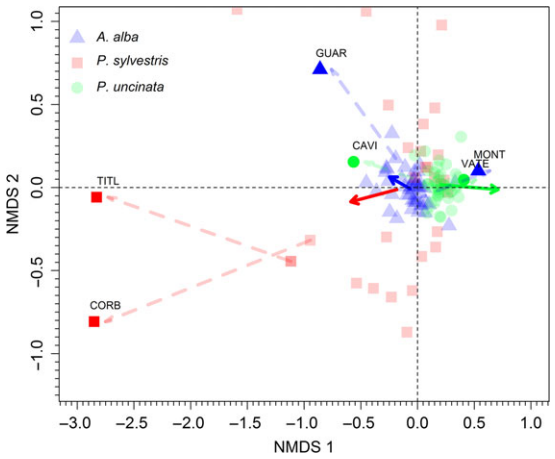


**Fig. 5** Scatter plots of the first two axes of a nonmetric multidimensional scaling (NMDS) showing the observed tree-ring width indices for all sites (symbols with light colors, 1950–2005 period) and the projected indices (symbols with dark colors, 2050–2100 period) for rear-edge sites (indicated with codes; see Fig. 1) considering the warmest emission scenario (RCP 8.5). Blue triangles, red squares and green circles correspond to silver fir (*Abies alba*), Scots pine (*Pinus sylvestris*) and mountain pine (*Pinus uncinata*) sites, respectively. The dark arrows show the expected changes in tree-ring width indices of all sites, while the light dashed arrows show the shift across the NMDS biplot considering only rear-edge stands. Stands located at rear-edge are indicated with dark color and labels (silver fir, GUAR and MONT sites; Scots pine, CORB and TITL sites; and Mountain pine, CAVI and VATE sites). [Colour figure can be viewed at wileyonlinelibrary.com].

We also observed that growth in other rear-edges may be strongly and negatively influenced by warming-induced drought stress (see also Gea-Izquierdo *et al.*, 2013). Warmer temperatures can increase potential evapotranspiration and drought stress during the growing season leading to dieback (McDowell *et al.*, 2008). These effects have already been observed in some of the studied rear-edge forests in the form of growth decline, forest dieback and rising mortality rates (Camarero *et al.*, 2015b). As similar episodes have been observed in different dry regions of southern and central Europe (Vacchiano *et al.*, 2012; Rigling *et al.*, 2013), our findings corroborate the predictions of increasing risk of drought-triggered dieback in similar drought-prone forests (Anderegg *et al.*, 2012).

### *Forest vulnerability to projected climate warming*

Based on climate projections of the process-based forward model of growth, the strongest temperature increases would cause many tree populations to shift from temperature- to moisture-limited growth, mainly at rear-edges and dry sites where the spring–summer conditions are close to the species' limits of climate tolerance (Fig. S5). The exact temperature and moisture thresholds should vary according to species and site conditions (Fig. 7). In general, climatic projections correspond to shorter growing seasons in silver fir and Scots pine but longer growing seasons in mountain pine. This would correspond to higher growth sensitivity to climate during the early growing season when warmer conditions could lead to a rapid melting of mountain snowpacks, increased evapotranspiration rates in low-elevation sites and thus drier conditions (Lavergne *et al.*, 2015). The forecasted longer dry season limitation would negatively affect the growth of silver fir and Scots pine (Fig. 6) by exceeding the functional thresholds for optimum growth responses ($gT$ and $gM$), especially on the dry species limits. In dry rear-edges, the lowest percentage of soil moisture under which growth is not limited ($M_2$) was lower in summer than in spring (Fig. 7), suggesting a prominent role of spring water deficit to growth as has been observed in xylogenesis studies (Camarero *et al.*, 2010). On the other hand, the minimum temperature threshold of growth ($T_1$) and the temperature at which growth is not limited ($T_2$) will increase for silver fir and Scots pine rear-edges (Table S6), thus experiencing more drought stress during the projected shorter growing season (Fig. 7). This is in line with studies emphasizing the dependence of wood formation on the duration and rate of cell production in the early growing period when drought stress is lower than in summer (Eilmann *et al.*, 2011; Cuny *et al.*, 2012). However, both Scots pine and silver fir may benefit from increased precipitation in fall if temperature is high enough (Gazol *et al.*, 2015; Sánchez-Salguero *et al.*, 2015). In contrast, in the case of mountain pine, only rear-edge sites showed a response to dry summer conditions in terms of growth reduction; for example, the VATE and CAVI sites presented the largest growth reductions of −10% under the RCP 8.5 scenario (Fig. 6). Furthermore, growth projections are characterized by warmer temperature thresholds extending the growing season during the second half of 21st century, thus enhancing the growth and productivity in mesic mountain pine forests as has been observed in the late 20th century (Galván *et al.*, 2012). These positive impacts on mountain pine tree growth in response to climate warming are predicted to occur at high-elevation forests often close to the uppermost Pyrenean forest limit. Cloudiness or a longer or deeper snowpack could greatly condition this growth improvement by reducing the growing season near the tree line (Lavergne *et al.*, 2015).

Every modeling approach has limitations, assumptions and handicaps. We chose this methodological framework because it is robust and provides results

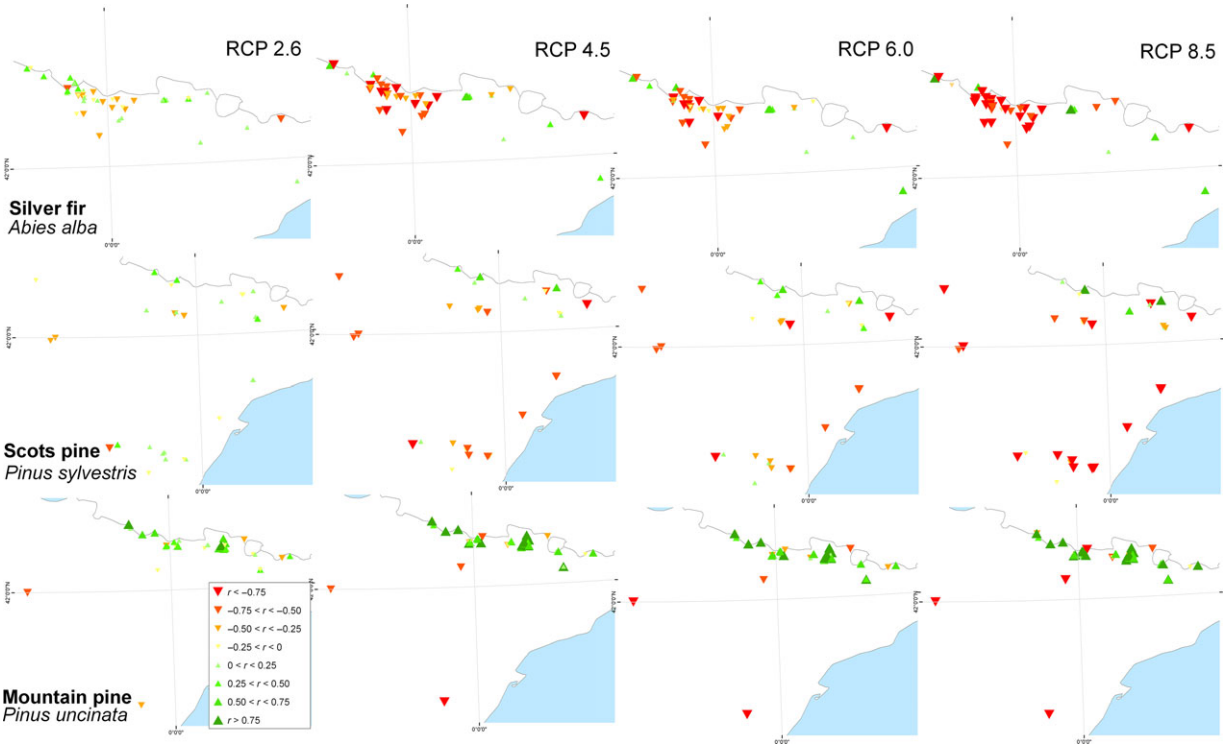


**Fig. 6** Maps displaying projected growth trends (Pearson correlation coefficients of site mean tree-ring width indices series) considering the 2001–2100 period following growth projections based on four IPCC AR5 emissions scenarios (from lowest to highest rates of warming: RCP 2.6, RCP 4.5, RCP 6.0 and RCP 8.5). Triangles pointing upward and downward indicate positive and negative trends, respectively. Values higher than 0.25 and lower than −0.25 are significant at $P < 0.05$. [Colour figure can be viewed at wileyonlinelibrary.com].

that are in accordance with what has been observed in field studies on forest vulnerability and climate-driven growth thresholds (Camarero *et al.*, 2015b). Nevertheless, process-based models show limitations because climate constrains other demographic processes than growth not considered in our study (e.g., regeneration, mortality; see Matías & Jump, 2015). We focused on radial growth, but primary growth and leaf phenology are also prominent components of forest productivity and leaf flushing is expected to advance due to climate warming (Vitasse *et al.*, 2011). Furthermore, extreme climatic events and biotic disturbances (e.g., cold or heat spells and insect outbreaks) could also play an important role in driving forest vulnerability to climate (Camarero *et al.*, 2015a; Ramming *et al.*, 2014). However, climate extremes are not fully represented by climate models and emission scenarios (IPCC, 2013). Several studies highlighted that the susceptibility of trees to extreme climatic events as droughts is generally expressed by low growth rates usually surpassing a critical minimum threshold (Bigler *et al.*, 2006; Camarero *et al.*, 2015b). This could be the case of silver fir forests which presented dieback after a sharp growth reduction in 1986 in some western rear-edge sites (Camarero *et al.*, 2011). Our projections indicate that such low growth conditions could be reached in the late 21st century (Fig. 4). Besides, the growth responses to climate could also be modulated by species-specific reactions to rising atmospheric $CO_2$ concentrations which could improve water-use efficiency and thus growth (Keenan *et al.*, 2011). Nevertheless, to the best of our knowledge, most studies have reported no growth improvements related to potential fertilization effects in the study area (Peñuelas *et al.*, 2008; Andreu-Hayles *et al.*, 2011; Camarero *et al.*, 2015c). Future fertilization effected cannot be discarded because tree species growing in the studied area have not experienced yet the range of $CO_2$ atmospheric concentrations projected by IPCC (2013) scenarios. Overall, the presented methodological framework provides an outlook for future improvements considering, for instance, the relevant role played by climate extremes.

On the other hand, due to the size trends of tree-ring width raw data and because of possible influences of nonclimatic disturbances, it was necessary to base our models on detrended TRWi (Williams *et al.*, 2010). We assume the potential bias caused using tree-ring width

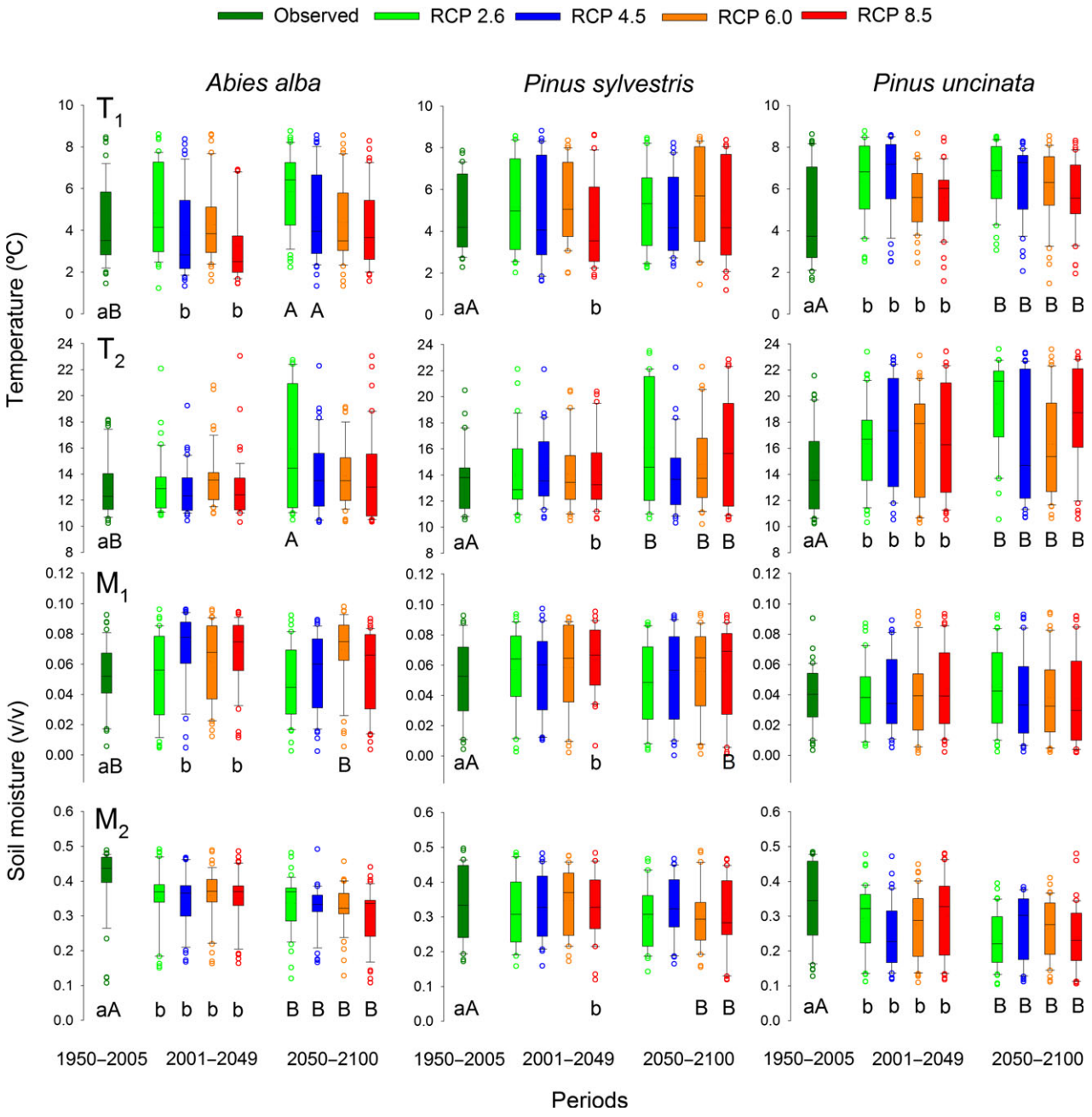


**Fig. 7** Statistics of the Bayesian estimation of the site-by-site tuned VS-Lite growth response parameters representing the temperature ($T_1$) or soil moisture ($M_1$) thresholds below which growth will not occur and the optimal temperature ($T_2$) or soil moisture parameters ($M_2$) above which growth is not limited by climate. Values correspond to the three study tree species (silver fir, *Abies alba*; Scots pine, *Pinus sylvestris*; and Mountain pine, *Pinus uncinata*), and parameters were fitted for the 1950–2005, 2001–2049 and 2050–2100 periods based on ensemble IPCC AR5 emission scenarios (RCP 2.6, RCP 4.5, RCP 6.0 and RCP 8.5). Different letters indicate significant ($P < 0.05$) differences between observed and projected periods based on Tukey's HSD *post hoc* tests (lowercase and uppercase letters correspond to the 2001–2049 and 2050–2100 periods, respectively). [Colour figure can be viewed at wileyonlinelibrary.com].

indices is small compared to the use of tree-ring width data because the applied detrending methods preserve much of the annual to decadal variations and led to comparable site chronologies (Laroque & Smith, 2003). Despite the aforementioned limitations, the high correlation values between simulated and measured TRWi series indicate that the VS-Lite model adequately reproduced interannual growth site variability (Fig. 4). For instance, showing the moisture limitations of rear-edge dry sites (including those of high-elevation

mountain pine forests) reduces the uncertainties associated with predictions of future forest vulnerability under a warmer climate.

The large intersite variability in modeled VS-Lite parameters (Fig. 7) may arise from differences in environmental conditions between sites or due to contrasting drought tolerances among tree populations caused by local adaptation and phenotypic plasticity (Valladares *et al*., 2014). In trees, the adjustment of anatomical and functional traits to environmental variability due to phenotypic plasticity and genetic variability is strong at the margins of the plants (Hampe, 2004), but the overall performance of a tree species may decline as the southernmost distributional limits are reached and vulnerability to climatic stress increases (Vergeer & Kunin, 2013). This could be the case for the southernmost studied tree populations located at the lowest elevations, which were most dependent on spring and early summer climate conditions. Tree species show adaptive features to increasing drought stress by adjusting their hydraulic system (e.g., leaf area to sapwood area ratio) and phenology to local climate, particularly those most widespread as Scots pine (Martínez-Vilalta *et al*., 2009) and silver fir (George *et al*., 2015). Our modeling approach could help to highlight locally adapted populations with traits providing drought tolerance and to derive predictions on future dieback events by mapping growth vulnerability. Identifying the responsible genetic controls of some of these traits will aid in conservation efforts of locally adapted range-edge tree populations which often represent unique genetic and phenotypic reservoirs (Sancho-Knapik *et al*., 2014; Rehm *et al*., 2015). This study advocates for actively preserving those rear-edge forests where vulnerability has been demonstrated by observations (late 20th-century dieback episodes) and projections (growth decline in the late 21st century) including actions still poorly evaluated in Europe as assisted migration (McLachlan *et al*., 2007).

To conclude, the use of a process-based growth model allowed us to define the vulnerability thresholds of forests by quantifying growth reactions to forecasted climate warming. The projected climate scenario corresponding to the most pronounced warming forecasted growth reduction in silver fir and Scots pine forests until 2050, whereas high-elevation mountain pine growth is projected to increase. Site variability often overrode these different responses between species because the most intense growth reduction was forecasted for some dry Scots pine and silver fir rear-edge populations. These predictions imply that climate warming would firstly lead to growth reduction in marginal populations, where a long-term decline in productivity could be used to portend impending dieback or local extinction.

## Acknowledgements

We acknowledge the use of the E-OBS climate dataset (EU-project ENSEMBLES) and the data providers in the ECA&D project (http://www.ecad.eu) and thank Dr. Geert Jan van Oldenborgh for his assistance. We also thank A. Hevia for help with statistical models. This study was supported by projects 387/2011 (OAPN, Spanish Ministry of Environment), CGL2011-26654 and CGL2015-69186-C2-1-R (Spanish Ministry of Economy). A. Gazol is supported by a Postdoctoral grant (MINECO-FPDI 2013-16600, FEDER funds). RSS and JCL were supported by the project CoMo-ReAdapt (CGL2013-48843-C2-1-R) and a postdoctoral fellowship to RSS (FEDER-Junta de Andalucía). We thank useful comments provided by D. Frank, the editor and three anonymous reviewers. The authors declare no conflict of interest.

## References

Allen CD, Breshears DD, McDowell NG (2015) On underestimation of global vulnerability to tree mortality and forest die-off from hotter drought in the Anthropocene. *Ecosphere*, **6**, 129.

Anchukaitis KJ, Evans MN, Kaplan A *et al*. (2006) Forward modeling of regional scale tree-ring patterns in the southeastern United States and the recent influence of summer drought. *Geophysical Research Letters*, **33**, L04705.

Anderegg WRL, Berry JA, Smith DD *et al*. (2012) The role of hydraulic and carbon stress in a widespread climate-induced forest die-off. *Proceedings of the National Academy of Sciences of the United States of America*, **109**, 233–237.

Anderegg WRL, Flint A, Huang C *et al*. (2015) Tree mortality predicted from drought-induced vascular damage. *Nature Geoscience*, **8**, 367–371.

Andreu L, Gutierrez E, Macias M *et al*. (2007) Climate increases regional tree-growth variability in Iberian pine forests. *Global Change Biology*, **13**, 1–12.

Andreu-Hayles L, Planells O, Gutiérrez E *et al*. (2011) Long tree-ring chronologies reveal 20th century increases in water-use efficiency but no enhancement of tree growth at five Iberian pine forests. *Global Change Biology*, **17**, 2095–2112.

Babst F, Poulter B, Trouet V *et al*. (2013) Site- and species-specific responses of forest growth to climate across the European continent. *Global Ecology and Biogeography*, **22**, 706–717.

Babst F, Alexander MR, Szejner P, Boriaud O, Klesse S *et al*. (2014) A tree-ring perspective on the terrestrial carbon cycle. *Oecologia*, **176**, 307–322.

Bigler C, Braker OU, Bugmann H, Dobbertin M, Rigling A (2006) Drought as an inciting mortality factor in Scots pine stands of the Valais, Switzerland. *Ecosystems*, **9**, 330–343.

Breitenmoser P, Brönnimann S, Frank D (2014) Forward modelling of tree-ring width and comparison with a global network of tree-ring chronologies. *Climate of the Past*, **10**, 437–449.

Camarero JJ, Guerrero-Campo J, Gutiérrez E (1998) Tree-ring structure and growth of *Pinus uncinata* Ram. and *Pinus sylvestris* L. in the Central Spanish Pyrenees. *Arctic and Alpine Research*, **30**, 1–10.

Camarero JJ, Olano JM, Parras A (2010) Plastic bimodal xylogenesis in conifers from continental Mediterranean climates. *New Phytologist*, **185**, 471–480.

Camarero JJ, Bigler C, Linares JC, Gil-Pelegrin E (2011) Synergistic effects of past historical logging and drought on the decline of Pyrenean silver fir forests. *Forest Ecology and Management*, **262**, 759–769.

Camarero JJ, Gazol A, Sancho-Benages S, Sanguesa-Barreda G (2015a) Know your limits? Climate extremes impact the range of Scots pine in unexpected places. *Annals of Botany*, **116**, 917–927.

Camarero JJ, Gazol A, Sangüesa-Barreda G, Oliva J, Vicente-Serrano SM (2015b) To die or not to die: early-warning signals of dieback in response to a severe drought. *Journal of Ecology*, **103**, 44–57.

Camarero JJ, Gazol A, Tardif JC, Conciatori F (2015c) Attributing forest responses to global-change drivers: limited evidence of a $CO_2$-fertilization effect in Iberian pine growth. *Journal of Biogeography*, **42**, 2220–2233.

Collins M, Knutti R, Arblaster J *et al*. (2014), Long-term climate change: projections, commitments and irreversibility. In: *Climate Change 2013 – The Physical Science Basis* (eds M Collins *et al*.), pp. 1029–1136, Cambridge University Press, Cambridge, UK.

Cook ER, Krusic P (2005) A tree-ring standardization program based on detrending and autoregressive time series modeling, with interactive graphics. Tree-Ring Laboratory, Lamont Doherty Earth Observatory, Columbia University, New York.

Cuny HE, Rathgeber CBK, Lebourgeois F, Fortin M, Fournier M (2012) Life strategies in intra-annual dynamics of wood formation: example of three conifer species in a temperate forest in north-east France. *Tree Physiology*, **32**, 612–625.

D'Amen M, Rahbek C, Zimmermann NE, Guisan A (2015) Spatial predictions at the community level: from current approaches to future frameworks. *Biological Reviews*. doi:10.1111/brv.12222.

Duveneck MJ, Scheller RM (2016) Measuring and managing resistance and resilience under climate change in northern Great Lake forests (USA). *Landscape Ecology*, **31**, 669–686.

Eilmann B, Zweifel R, Buchmann N, Pannatier EG, Rigling A (2011) Drought alters timing, quantity, and quality of wood formation in Scots pine. *Journal of Experimental Botany*, **62**, 2763–2771.

Evans MN, Reichert BK, Kaplan A *et al.* (2006) A forward modeling approach to paleoclimatic interpretation of tree-ring data. *Journal of Geophysical Research*, **111**, G03008.

Fritts HC (2001) *Tree Rings and Climate*. Blackburn Press, Caldwell, London.

Galiano L, Martínez-Vilalta J, Lloret F (2011) Drought-induced multifactor decline of Scots Pine in the Pyrenees and potential vegetation change by the expansion of co-occurring oak Species. *Ecosystems*, **13**, 978–991.

Galván JD, Camarero JJ, Sangüesa-Barreda G, Alla AQ, Gutiérrez E (2012) Sapwood area drives growth in mountain conifer forests. *Journal of Ecology*, **100**, 1233–1244.

García-Valdés R, Gotelli NJ, Zavala MA, Purves DW, Araújo MB (2015) Effects of climate, species interactions, and dispersal on decadal colonization and extinction rates of Iberian tree species. *Ecological Modelling*, **309**, 118–127.

Gazol A, Camarero JJ, Gutiérrez E *et al.* (2015) Distinct effects of climate warming on populations of silver fir (*Abies alba*) across Europe. *Journal of Biogeography*, **42**, 1150–1162.

Gea-Izquierdo G, Fernández de Uña L, Cañellas I (2013) Growth projections reveal local vulnerability of Mediterranean oaks with rising temperatures. *Forest Ecology and Management*, **305**, 282–293.

George JP, Schueler S, Karanitsch-Ackerl S *et al.* (2015) Inter- and intra-specific variation in drought sensitivity in *Abies* species and its relation to wood density and growth traits. *Agricultural and Forest Meteorology*, **214–215**, 430–443.

Giorgi F, Lionello P (2008) Climate change projections for the Mediterranean region. *Global and Planetary Change*, **63**, 90–104.

Guada G, Camarero JJ, Sánchez-Salguero R, Navarro-Cerrillo RM (2016) Limited growth recovery after drought-induced forest dieback in very defoliated trees of two pine species. *Frontiers in Plant Science*, **7**, 418.

Guiot J, Boucher E, Gea-Izquierdo G (2014) Process models and model-data fusion in dendroecology. *Frontiers in Ecology and Evolution*, **2**, 52.

Hampe A (2004) Bioclimate envelope models: what they detect and what they hide. *Global Ecology and Biogeography*, **13**, 469–471.

Hampe A, Petit RJ (2005) Conserving biodiversity under climate change: the rear edge matters. *Ecology Letters*, **8**, 461–467.

Haylock MR, Hofstra N, Klein Tank AMG *et al.* (2008) A European daily high-resolution gridded dataset of surface temperature and precipitation. *Journal of Geophysical Research: Atmospheres*, **113**, D20119.

Holmes RL (1983) Computer-assisted quality control in tree-ring dating and measurement. *Tree-Ring Bulletin*, **43**, 68–78.

Huang J, van den Dool HM, Georgakakos KP (1996) Analysis of model-calculated soil moisture over the United States (1931–1993) and applications to long-range temperature forecasts. *Journal of Climate*, **9**, 1350–1362.

Huang J-G, Bergeron Y, Berninger F *et al.* (2013) Impact of future climate on radial growth of four major boreal tree species in the Eastern Canadian boreal forest. *PLoS One*, **8**, e56758.

IPCC (2013) Climate change 2013: the physical science basis. In: *Contribution of Working Group I to the Fifth Assessment Report of the Intergovernmental Panel on Climate Change* (eds Stocker TF, Qin D, Plattner G-K, Tignor M, Allen SK, Boschung J, Nauels A, Xia Y, Bex V, Midgley PM), 1535 pp. Cambridge University Press, Cambridge, UK and New York, USA.

Keenan T, Maria-Serra J, Lloret F, Ninyerola M, Sabate S (2011) Predicting the future of forests in the Mediterranean under climate change, with niche- and process-based models: $CO_2$ matters!. *Global Change Biology*, **17**, 565–579.

Laroque CP, Smith DJ (2003) Radial-growth forecasts for five high-elevation conifer species on Vancouver Island, British Columbia. *Forest Ecology and Management*, **183**, 313–325.

Lavergne A, Daux V, Villalba R, Barichivich J (2015) Temporal changes in climatic limitation of tree-growth at upper treeline forests: contrasted responses along the west-to-east humidity gradient in Northern Patagonia. *Dendrochronologia*, **36**, 49–59.

Lelieveld J, Proestos Y, Hadjinicolaou P *et al.* (2016) Strongly increasing heat extremes in the Middle East and North Africa (MENA) in the 21st century. *Climatic Change*, **137**, 245–260.

Linares JC, Camarero JJ (2012a) Growth patterns and sensitivity to climate predict silver fir decline in the Spanish Pyrenees. *European Journal of Forest Research*, **131**, 1001–1012.

Linares JC, Camarero JJ (2012b) From pattern to process: linking intrinsic water-use efficiency to drought induced forest decline. *Global Change Biology*, **18**, 1000–1015.

Lindner M, Maroschek M, Netherer S *et al.* (2010) Climate change impacts, adaptive capacity, and vulnerability of European forest ecosystems. *Forest Ecology and Management*, **259**, 698–709.

Lloret F, Martinez-Vilalta J, Serra-Diaz JM, Ninyerola M (2013) Relationship between projected changes in future climatic suitability and demographic and functional traits of forest tree species in Spain. *Climatic Change*, **120**, 449–462.

Macias M, Andreu L, Bosch O, Camarero JJ, Gutiérrez E (2006) Increasing aridity is enhancing silver fir (*Abies alba* Mill.) water stress in its south-western distribution limit. *Climatic Change*, **79**, 289–313.

Martin-Benito D, Pederson N (2015) Convergence in drought stress, but a divergence of climatic drivers across a latitudinal gradient in a temperate broadleaf forest. *Journal of Biogeography*, **42**, 925–937.

Martínez-Vilalta J, Cochard H, Mencuccini M *et al.* (2009) Hydraulic adjustment of Scots pine across Europe. *New Phytologist*, **184**, 353–364.

Martínez-Vilatla J, Piñol J (2002) Drought-induced mortality and hydraulic architecture in pine populations of the NE Iberian Peninsula. *Forest Ecology and Management*, **161**, 247–256.

Matías L, Jump AS (2015) Asymmetric changes of growth and reproductive investment herald altitudinal and latitudinal range shifts of two woody species. *Global Change Biology*, **21**, 882–896.

McDowell NG, Pockman WT, Allen CD *et al.* (2008) Mechanisms of plant survival and mortality during drought: why do some plants survive while others succumb to drought? *New Phytologist*, **178**, 719–739.

McLachlan JS, Hellmann JJ, Schwartz MW (2007) A framework for debate of assisted migration in an era of climate change. *Conservation Biology*, **21**, 297–302.

Mina M, Martin-Benito D, Bugmann H, Cailleret M (2016) Forward modeling of tree-ring width improves simulation of forest growth responses to drought. *Agricultural and Forest Meteorology*, **221**, 13–33.

Moreno A, Hasenauer H (2016) Spatial downscaling of European climate data. *International Journal of Climatology*, **36**, 1444–1458.

Nehrbass-Ahles C, Babst F, Klesse S *et al.* (2014) The influence of sampling design on tree-ring-based quantification of forest growth. *Global Change Biology*, **20**, 2867–2885.

Oberhuber W (2004) Influence of climate on radial growth of *Pinus cembra* within the alpine timberline ecotone. *Tree Physiology*, **24**, 291–301.

Pearson RG, Dawson TP (2003) Predicting the impacts of climate change on the distribution of species: are bioclimate envelope models useful? *Global Ecology and Biogeography*, **12**, 361–371.

Peñuelas J, Hunt JM, Ogaya R, Jump AS (2008) Twentieth century changes of tree-ring delta $^{13}C$ at the southern range-edge of *Fagus sylvatica*: increasing water-use efficiency does not avoid the growth decline induced by warming at low altitudes. *Global Change Biology*, **14**, 1076–1088.

Pinheiro J, Bates D, DebRoy S, Sarkar D (2009) *nlme: Linear and Nonlinear Mixed Effects Models*. R package version 3.1-96. Available at: http://cran.r-project.org/web/packages/nlme/index.html. (accessed 13 April 2016).

R Development Core Team (2016) *R: A Language and Environment for Statistical Computing*. R Foundation for Statistical Computing, Vienna, Austria. Available at: http://www.r-project.org/. (accessed 13 April 2016).

Ramming A, Wiedermann M, Donges JF *et al.* (2014) Tree-ring responses to extreme climate events as benchmarks for terrestrial dynamic vegetation models. *Biogeosciences Discussions*, **11**, 2537–2568.

Rehm EM, Olivas P, Stroud J, Feeley KJ (2015) Losing your edge: climate change and the conservation value of range-edge populations. *Ecology and Evolution*, **5**, 4315–4326.

Rigling A, Bigler C, Eilmann B *et al.* (2013) Driving factors of a vegetation shift from Scots pine to pubescent oak in dry Alpine forests. *Global Change Biology*, **19**, 229–240.

Ruosch M, Spahni R, Joos F *et al.* (2016) Past and future evolution of *Abies alba* forests in Europe – comparison of a dynamic vegetation model with palaeo data and observations. *Global Change Biology*, **22**, 727–740.

Sánchez-Salguero R, Navarro-Cerrillo RM, Camarero JJ, Fernández-Cancio A (2012) Selective drought-induced decline of pine species in southeastern Spain. *Climatic Change*, **113**, 767–785.

Sánchez-Salguero R, Camarero JJ, Hevia A *et al.* (2015) What drives growth of Scots pine in continental Mediterranean climates: drought, low temperatures or both? *Agricultural and Forest Meteorology*, **206**, 151–162.

Sancho-Knapik D, Peguero-Pina J, Cremer E *et al.* (2014) Genetic and environmental characterization of *Abies alba* Mill. populations at its western rear edge. *Pirineos*, **169**, e007.

Serra-Díaz JM, Keenan TF, Ninyerola M, Sabaté S, Gracia C, Lloret F (2013) Geographical patterns of congruence and incongruence between correlative species distribution models and a process-based ecophysiological growth model. *Journal of Biogeography*, **40**, 1928–1938.

Shestakova TA, Gutiérrez E, Kirdyanov AV *et al.* (2016) Forests synchronize their growth in contrasting Eurasian regions in response to climate warming. *Proceedings of the National Academy of Sciences of the United States of America*, **113**, 662–667.

Tardif J, Camarero JJ, Ribas M, Gutiérrez E (2003) Spatiotemporal variability in tree ring growth in the Central Pyrenees: climatic and site influences. *Ecological Monographs*, **73**, 241–257.

Taylor KE, Stouffer RJ, Meehl GA (2012) An overview of CMIP5 and the experiment design. *Bulletin of the American Meteorological Society*, **93**, 485–498.

Tolwinski-Ward SE, Evans MN, Hughes MK, Anchukaitis KJ (2011) An efficient forward model of the climate controls on interannual variation in tree-ring width. *Climate Dynamics*, **36**, 2419–2439.

Tolwinski-Ward SE, Anchukaitis KJ, Evans MN (2013) Bayesian parameter estimation and interpretation for an intermediate model of tree-ring width. *Climate of the Past*, **9**, 1481–1493.

Touchan R, Shishov VV, Meko DM, Nouiri I, Grachev A (2012) Process based model sheds light on climate sensitivity of Mediterranean tree-ring width. *Biogeosciences*, **9**, 965–972.

Vacchiano G, Garbarino M, Borgogno Mondino E, Motta R (2012) Evidences of drought stress as a predisposing factor to Scots pine decline in Valle d'Aosta (Italy). *European Journal of Forest Research*, **131**, 989–1000.

Vaganov EA, Hughes MK, Shashkin AV (2006) *Growth Dynamics of Conifer Tree Rings*. Springer, Berlin.

Vaganov EA, Anchukaitis KJ, Evans MN (2011) How well understood are the processes that create dendroclimatic records? A mechanistic model of the climatic control on conifer tree-ring growth dynamics. In: *Dendroclimatology. Developments in Paleoenvironmental Research* (eds Hughes MK, Swetnam TW, Diaz HF). pp. 37–75. Springer, ???, the Netherlands.

Valladares F, Matesanz FS, Guilhaumon F *et al.* (2014) The effects of phenotypic plasticity and local adaptation on forecasts of species range shifts under climate change. *Ecology Letters*, **17**, 1351–1364.

Van Vuuren DP, Edmonds J, Kainuma M *et al.* (2011) The representative concentration pathways: an overview. *Climatic Change*, **109**, 5–31.

Vergeer P, Kunin WE (2013) Adaptation at range margins: common garden trials and the performance of *Arabidopsis lyrata* across its northwestern European range. *New Phytologist*, **197**, 989–1001.

Vigo J, Ninot JM (1987) *Los Pirineos*. In: *La vegetación de España* (eds Peinado-Lorca M, Rivas-Martínez S), pp. 351–384. Publicaciones Universidad Alcalá de Henares, Alcalá de Henares.

Vitasse Y, Franc C, Delpierre N, Dufrêne E, Kremer A, Chuine I, Delzon S (2011) Assessing the effects of climate change on the phenology of European temperate trees. *Agricultural and Forest Meteorology*, **151**, 969–980.

Way DA, Oren R (2010) Differential responses to changes in growth temperature between trees from different functional groups and biomes: a review and synthesis of data. *Tree Physiology*, **30**, 669–688.

Williams AP, Michaelsen J, Leavitt SW, Still CJ (2010) Using tree rings to predict the response of tree growth to climate change in the continental United States during the twenty-first century. *Earth Interactions*, **14**, 1–20.

Williams AP, Allen CD, Macalady AK *et al.* (2013) Temperature as a potent driver of regional forest drought stress and tree mortality. *Nature Climate Change*, **3**, 292–297.

Zhu K, Woodall CW, Clark JS (2012) Failure to migrate: lack of tree range expansion in response to climate change. *Global Change Biology*, **18**, 1042–1052.

## Supporting Information

Additional Supporting Information may be found in the online version of this article:

**Figure S1.** Maps of the sampled sites for *Abies alba*, silver fir; *Pinus sylvestris*, Scots pine; and *Pinus uncinata*, Mountain pine.
**Figure S2.** Mean annual temperature and annual precipitation patterns and trends.
**Figure S3.** Climate projections according to the RCPs emission scenarios (IPCC, 2013).
**Figure S4.** Maps displaying Pearson correlation between observed site series (TRWi) and VS-Lite model indices (TRWi-$_{VSL}$).
**Figure S5.** Simulated and projected monthly growth response curves ($gT$, $gM$) for the period 1950–2005 and IPCC AR5 emission scenarios. Selected rear-edges stands are shown.
**Figure S6.** VS-Lite growth parameters ($T_1$, $T_2$, $M_1$, and $M_2$) trends with elevation, longitude and latitude.
**Figure S7.** Observed (TRWi) and projected (TRWi$_p$) mean tree-ring width indices for each tree species.
**Figure S8.** Scatter plots of a Non-Metric Multidimensional Scaling (NMDS) analysis considering observed (TRWi), VS-Lite modeled (TRWi-$_{VSL}$) and projected (TRWi$_p$) tree-ring width indices.
**Table S1.** Main characteristics of sampled sites.
**Table S2.** Summary of dendrochronological statistics.
**Table S3.** Pearson's correlation coefficients calculated between observed (TRWi) and VS-Lite projected (TRWi-$_{VSL}$) tree-ring width indices.
**Table S4.** Statistics of the Bayesian estimation of VS-Lite growth response parameters for the period 1950–2005.
**Table S5.** Summary of Generalized Least Squares regressions models.
**Table S6.** Statistics of the Bayesian estimation of VS-Lite growth response parameters for the 21st century.